Impact of HPMCAS Grade on the Release of Weakly Basic Drugs from Amorphous Solid Dispersions

Pradnya Bapat, Lynne S. Taylor[1]*

Department of Industrial and Molecular Pharmaceutics, College of Pharmacy, Purdue University, West Lafayette, Indiana 47907, United States

*Correspondence: Lynne S. Taylor

Telephone: +1-765-496-6614; Fax: +1-765-494-6545

Email address: lstaylor@purdue.edu

1. Abstract

Oppositely charged species can form electrostatic interactions in aqueous solution, and these may lead to reduced solubility of the interacting components. Herein, insoluble complex formation between the lipophilic weakly basic drugs, cinnarizine or loratadine, and the enteric polymer, hydroxypropyl methylcellulose acetate succinate (HPMCAS), was studied and used to better understand drug and polymer release from their corresponding amorphous solid dispersions (ASDs). Surface area normalized release experiments were performed at various pH conditions for three different grades of HPMCAS, LF, MF and HF, as well as their ASDs. Both polymer and drug release rates were measured for the ASDs. Complexation tendency was evaluated by measuring the extent of polymer loss from the aqueous phase in the presence of the drug. Results showed that release from ASDs with HPMCAS-LF was less impacted by the presence of a cationic form of the drug than ASDs prepared with the HF grade. Furthermore, an increase in pH, leading to a reduction in the extent of ionized drug also led to an improvement in release rate. These observations provide a baseline to understand the role of drug-polymer electrostatic interactions on release from ASDs formulated with HPMCAS. Future studies should focus on adding complexity to media conditions by employing simulated intestinal fluids with solubilizing components.

Keywords: electrostatic interactions; critical ionization extent; solubility; pH

TOC Graphic

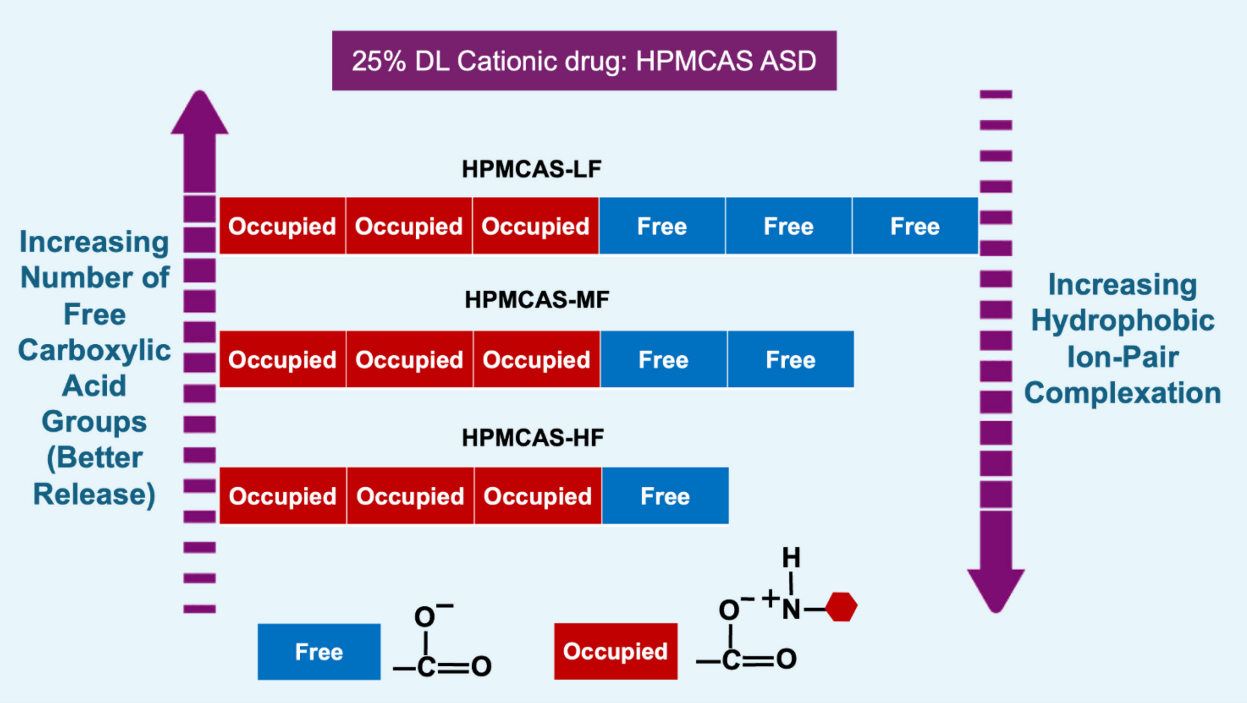
25% DL Cationic drug: HPMCAS ASD
HPMCAS-LF
Occupied
Occupied
Occupied
Free
Free
Free
HPMCAS-MF
Occupied
Occupied
Occupied
Free
Free
HPMCAS-HF
Occupied
Occupied
Occupied
Free
Increasing Number of Free Carboxylic Acid Groups (Better Release)
Increasing Hydrophobic Ion-Pair Complexation
Free
Occupied

2. Introduction

Amorphous solid dispersion (ASD) is an effective formulation strategy to improve the release rate and achievable solution concentrations of poorly water soluble new chemical entities (NCEs).[1–8] The amorphous form of a drug can achieve a higher apparent solubility compared to the crystalline form. However, formulation as an ASD by combining with a polymer, rather than using the neat amorphous form, is typically necessary. This is due to the instability of the neat amorphous drug that arises from its high free energy and tendency to convert to a more stable crystalline form.[9–14] To exploit the apparent solubility advantage of an amorphous drug, the properties of the polymer used to formulate the ASD are critical. The polymer aids in crystallization inhibition and also improves the drug release rate.[3,15–25] Improvements in drug release rate are linked to the higher solubility of the polymer relative to the drug, and hence, when the drug release rate is coupled to that of the polymer, drug release is enhanced. Congruent release of drug and polymer from the ASD is thus observed when the release is controlled by the polymer.[15,26–36] Hydroxypropyl methylcellulose acetate succinate (HPMCAS) is a commonly-used ASD polymer, in particular when the ASD is prepared by spray drying.[3,6,37–41] Considering the critical role played by the polymer in determining the subsequent ASD performance, a deeper understanding of polymer dissolution from ASDs is important.[42] In particular, the impact of molecularly dispersed drug on polymer release remains a largely unexplored area. Congruent release for HPMCAS-based ASDs has been observed for some drug loading regimens,[43–45] and the critical ionization fraction model has been invoked for conceptual understanding of release rates of acidic polymers that are insoluble at low pH.[45,46] According to this model, for polymer dissolution to commence, it is not necessary for every COOH (or other ionizable) group in the entire polymer to ionize. Rather there is a critical fraction of groups that need to ionize before

dissolution starts, and after reaching this fraction, the rate increases with the extent of ionization beyond this fraction. Ionization (to carboxylate ions in the case of HPMCAS) leads to enhanced hydration, plasticization, and dilution, allowing for the subsequent dissolution of polymer chains. Any hindrance to polymer hydration, e.g. by a hydrophobic drug strongly interacting with the carboxylate ion in the ASD can impact its solubility and dissolution rate. Different grades of HPMCAS, namely HPMCAS-LF, HPMCAS-MF and HPMCAS-HF have been investigated in ASD formulations.[4,7,13,14,23,38,39,41,47–54] These studies have centered on evaluating the impact of HPMCAS polymer grade on crystallization inhibition, and the formation and properties of the drug-rich nanodroplets formed following ASD dissolution. There have been fewer studies evaluating the role of HPMCAS grade on release kinetics. Bapat et al.[3] recently studied the impact of various weak acid, neutral, and weak base drugs on the release performance of ASDs with HPMCAS-MF and highlighted the importance of studying drug-polymer interactions. They observed that weakly basic drugs that were cationic at the dissolution pH released poorly from HPMCAS-MF ASDs, and this was attributed to the formation of hydrophobic ion pairs via electrostatic interactions between the drug and polymer leading to a reduction in polymer hydration.

The various HPMCAS grades have different absolute amounts as well as ratios of succinoyl (ionizable and hydrophilic) and acetyl (hydrophobic) groups, with LF having highest extent of succinoyl groups whereas HF has highest amount of acetyl groups.[13,40,41,49,50,55–58] The impact of ionic interactions with lipophilic cationic drugs on ASD release performance is expected to vary between the different HPMCAS grades, but has been little explored. Herein, it was hypothesized that at equivalent drug loadings, a lipophilic cation would impair the release performance of

ASDs with the HF grade to a greater extent than those prepared with the MF grade, while the LF grade of HPMCAS would result in ASDs with the best performance.

To test this hypothesis, two drugs, loratadine and cinnarizine, were chosen as model lipophilic, weakly basic drugs. Loratadine is partially cationic and cinnarizine is fully cationic at a dissolution pH of 6.8. ASDs with HPMCAS, -LF, -MF and -HF grades were prepared with loratadine and cinnarizine. Surface-area normalized release studies were performed at two pH values to vary the ionization state of the drug. Potentiometric titration was utilized to quantitate the acid content of the different grades. Complexation experiments were performed between drugs and with different polymer grades.

3. Materials

Loratadine (LOR) was purchased from Attix Pharmaceuticals (Toronto, ON, Canada). Cinnarizine (CNZ) was supplied by Alfa Aesar (Ward Hill, MA, USA). Hydroxypropyl methyl cellulose acetate succinate (HPMCAS AQOAT-MF, HPMCAS AQOAT-LF, HPMCAS AQOAT-HF) was supplied by Shin-Etsu (Tokyo, Japan). The structures of LOR, CNZ and HPMCAS are shown in Figure 1. Ethanol (EtOH), methanol (MeOH), dichloromethane (DCM), hydrochloric acid (HCl), formic acid (FA), acetonitrile (ACN), tetrahydrofuran (THF), sodium hydroxide (NaOH), sodium phosphate dibasic anhydrous (Na_2HPO_4), sodium phosphate monobasic monohydrate ($NaH_2PO_4.H_2O$) were purchased from Fischer Chemicals (Fair Lawn, NJ, USA). Buffer compositions are detailed in Table S1.

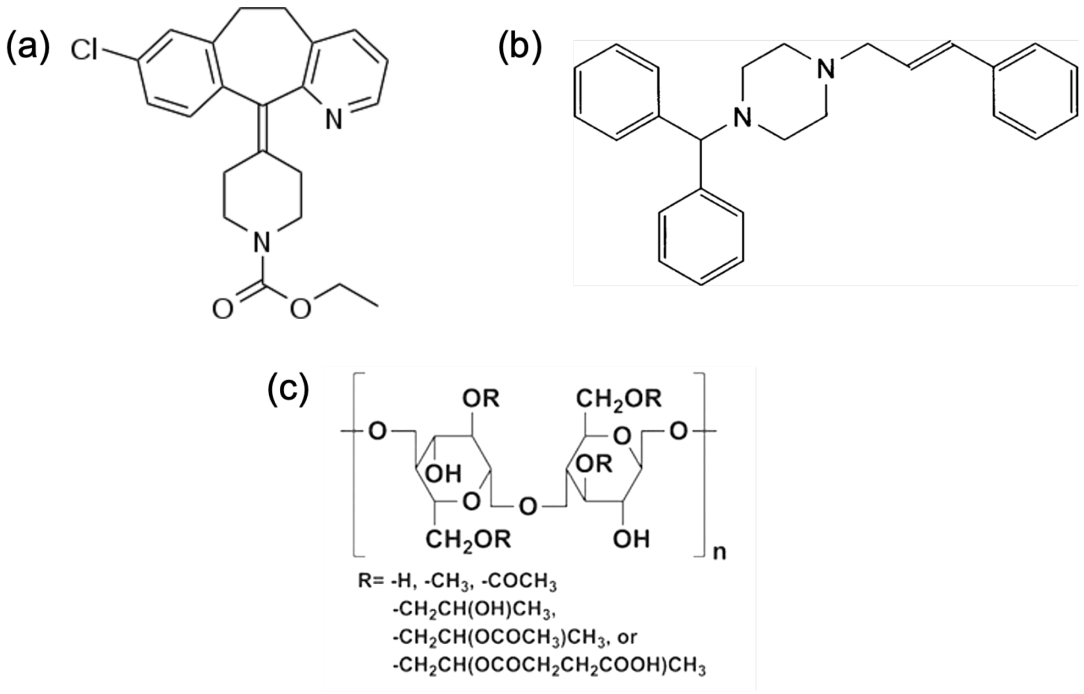

Figure 1. Chemical structures of (a) loratadine (LOR), (b) cinnarizine (CNZ), and (c) hydroxypropyl methyl cellulose acetate succinate (HPMCAS)

4. Methods

4.1. High Performance Liquid Chromatography (HPLC) Analysis of Drugs

For analysis of both LOR and CNZ, an Ascentis® Express (Sigma-Aldrich, St. Louis, MO) 90 Å C18 column with dimensions of 15 cm × 4.6 mm and particle size of 5 µm was used. For HPLC analysis of LOR, 0.1% TFA in water and ACN in 60:40 v/v was used as the mobile phase at a 1 mL/min flow rate, with an injection volume of 50 µL and ultraviolet (UV) detection wavelength at 210 nm. For CNZ HPLC analysis, 0.1% TFA in water and ACN in 30:70 v/v was used as the mobile phase at a 0.5 mL/min flow rate, with an injection volume of 30 µL and UV detection wavelength at 251 nm. Calibration curves were prepared in triplicate in the concentration range of 1-50 µg/mL with an R^2 of 0.999.

4.2. Analysis of HPMCAS

For analysis of HPMCAS concentration from surface normalized dissolution of ASDs, HPLC with an evaporative light scattering detector (ELSD) and a Shodex RS pak DS-413 column were used. 0.1% FA in water and 0.1% FA in ACN was used as the mobile phase with a gradient maintained at 0.5 mL/min flow rate, an injection volume of 80 µL and UV detection at 205 nm. A continuous flow of high-pressure nitrogen at a rate of 1.5 standard L/min was maintained to the ELSD detector. The nebulizer temperature was set to 80 ºC and the evaporator temperature was set to 85 ºC. The details of the gradient method are summarized in Table S2. Calibration curves were prepared in triplicate in the concentration range of 1-250 µg/mL with an R^2 of 0.999.

For analysis of HPMCAS concentration from complexation experiments, a colorimetric method was used. Briefly, 10 µL of phenol (4 g dissolved in 1 mL of water) and 1 mL of sulfuric acid were added to 400 µL of sample and vortexed for 5 s. The sample was left for color development and the absorbance was collected using a Varian Cary 300 Bio (Varian, Inc., Palo Alto, CA, USA) UV-visible spectrophotometer at 490 nm. Calibration curves were prepared over the concentration range of 1-100 µg/mL with R^2 of 0.999.

4.3. Preparation of Amorphous Solid Dispersions

HPMCAS-based ASDs of loratadine and cinnarizine at 25% drug loading (DL) with different grades of HPMCAS (LF, MF, HF) were prepared by rotary evaporation. Briefly, drug and polymer were dissolved in 1: 2 v/v methanol and dichloromethane and the solvent was evaporated using a rotary evaporator (Hei-VAP Core rotary evaporator, Heidolph Instruments, Schwabach, Germany) equipped with an Ecodyst EcoChyll S cooler (Ecodyst, Apex, NC, USA) using a water bath maintained at 50 °C. After rotary evaporation, ASDs were kept under vacuum overnight to remove excess solvent. ASDs were then cryomilled using a 6750 Freezer/Mill

(SPEX SamplePrep, Metuchen, NJ) and the ASD powder was passed through sieves, retaining the 106-250 μm particle size sieve cut. ASDs were confirmed to be amorphous using powder X-ray diffraction (PXRD) and polarized light microscopy (PLM).

4.4. Surface Area Normalized Dissolution Rate Experiments

Rotating disc, surface area normalized release experiments for neat polymers and ASDs were performed using Wood's apparatus (Agilent Technologies, Santa Clara, CA). Briefly, 100 mg of the sample was weighed and added to an 8 mm die, followed by compression using a Carver press (Carver, Wabash, IN) at 1500 psi held for one minute. Buffer was added to a jacketed beaker connected to a water bath maintained at 37 °C. Only one surface of the die, which was attached to the spindle rotating at 100 rpm, was exposed to the buffer. The experiment was performed for 60 min with samples taken at 5, 10, 15, 20, 25, 30, 40, 50 and 60 min, followed by replenishment with fresh media. The pH of the medium was checked at the end of the experiment and was found to be maintained at the target pH ± 0.1. The samples were analyzed using HPLC to quantify drug and polymer using methods developed previously.[3] The normalized release rate was calculated from eq. 1.

$$R = \frac{k \times V}{S \times x} \qquad \text{(eq. 1)}$$

where k is the slope of the regression line of a plot of solution concentration versus time, V is the volume of dissolution medium (100 mL), S is the surface area of the die exposed to the dissolution medium (0.5 cm^2) and x is the weight fraction of the component of interest.

4.5. Potentiometric Titrations

The method to perform potentiometric titrations was adapted from Hiew et al.[45] Briefly, HPMCAS-LF and HPMCAS-HF were dried in an oven at 105 °C for 30 min to remove residual water. Oven dried polymers were then stored under vacuum overnight. The dried polymer was

then weighed, dispersed in HPLC grade ultrapure water and stirred. To dissolve the polymer completely, 260 μL of 0.5 M NaOH was added and the solution was stirred for 24 h. The pH of the solution was measured using a B10P benchtop pH meter (VWR International, Radnor, PA) with a connected SympHony combination pH probe (VWR International, Radnor, PA). 0.1 N HCl was added in small increments to generate the titration curves. The pH probe was left in the vial for continuous measurement throughout the experiment. The first end point in the titration curves represents neutralization of excess NaOH added to the polymer solution. The second end point represents precipitation of all of the polymer. The difference between the amount of 0.1 N HCl required for first and second end points is directly proportional to the amount of -COOH groups present in the polymer. The pK_a values for the different polymer grades were considered to be indicated as the half neutralization points. End points were calculated by fitting at least five equilibration points to a polynomial equation using the curve fitting app in MATLAB (The MathWorks, MA). In the plot of second derivative ($\Delta(\Delta pH)/\Delta V2$) vs volume of the titrant added, the point where the second derivative crosses the abscissa was considered as the end point.

4.6. Complexation Experiments

Complexation experiments were performed to measure interactions between the model drugs and the LF or HF grades of HPMCAS in solution that led to an insoluble precipitate. Briefly, three stock solutions were prepared, viz., neat drug dissolved in THF, neat polymer dissolved in THF (52.5 mg/mL) and drug: polymer dissolved in THF with the polymer concentration fixed at 52.5 mg/mL. A small aliquot of each stock solution was then added to pH 6.0 phosphate buffer with continuous stirring. The concentration of THF added to buffer ranged from 10-15 μL/mL. The drug stock solution was added to the buffer to achieve a concentration above its amorphous solubility and the polymer stock solution was added to achieve a concentration of 0.5 mg/mL,

which is far below its solubility limit of 4-8 mg/mL in pH 6.0 phosphate buffer.[43] Additional details about the drug and polymer concentrations achieved in each solution during complexation experiment are shown in Table 1. When the neat drug stock solution was added to buffer, the drug precipitated, forming a turbid solution. This was then centrifuged at 14800 rpm using a Sorvall Legend Micro 21R centrifuge (Thermo Scientific, Waltham, MA) to generate a pellet and supernatant. The pellet was later assayed to confirm it was comprised of drug. When neat HPMCAS stock solution was added to buffer, the polymer dissolved completely and after centrifugation no pellet formed. When the third stock solution containing both drug and polymer was added to buffer with continuous stirring, the solution turned turbid. The solution was centrifuged to generate a pellet and supernatant. The presence of polymer in the pellet indicated the formation of an insoluble complex since the equivalent concentration of polymer in the absence of drug was soluble. The percent polymer complexed with the drug was calculated by measuring the concentration of the polymer in the supernatant using following equation:

$$\%\ Polymer\ complexed = \left(1 - \frac{Polymer\ in\ the\ supernatant}{Total\ polymer\ in\ the\ solution}\right) \times 100 \qquad \text{(eq. 2)}$$

Table 1. Details of complexation method at various drug: polymer molar ratios.

Drug	Polymer grade	Drug: polymer molar ratio	Amount of -COOH groups (mmol/g)	Polymer concentration in solution (µg/mL)	Drug concentration in solution (µg/mL)
Cinnarizine (CNZ)	LF	0.25:1	1.52 ± 0.03	500	75
		0.5:1			150
		0.75:1			225
		1:1			300
	HF	0.25:1	0.76 ± 0.02		
		0.5:1			
		0.75:1			
		1:1			150
Loratadine (LOR)	LF	1:1	1.52 ± 0.03		300
	HF	1:1	0.76 ± 0.02		150

4.7. Equilibrium Slurry pH Measurement

Equilibrium surface pH of HPMCAS-LF and HPMCAS-HF suspensions was estimated using the slurry pH method developed by Pudipeddi et al.[59] Briefly, an excess amount of polymer was dispersed in ultrapure water and stirred overnight to prepare a saturated solution. The pH of the polymer suspension was measured using a B10P benchtop pH meter (VWR International, Radnor, PA) with a connected SympHony combination pH probe (VWR International, Radnor, PA). The pH for all slurries equilibrated within 15 minutes indicating the solutions were saturated in terms of their pH. The final equilibrated pH value are taken to represents the lowest possible surface pH of the polymer during dissolution.

5. Results

5.1. Surface Area Normalized Dissolution Rate Experiments

Figure 2 shows surface area normalized release rates of neat HPMCAS LF, MF and HF grades in 50 mM pH 6.8 phosphate buffer (Figure 2a) and in 50 mM pH 7.5 phosphate buffer (Figure 2b). The intrinsic dissolution rate (IDR) of each grade was higher at pH 7.5 than at pH 6.8. LF showed the highest IDR followed by MF and then by HF at both pH conditions. LF IDR was approximately three-fold faster than HF at both pH conditions.

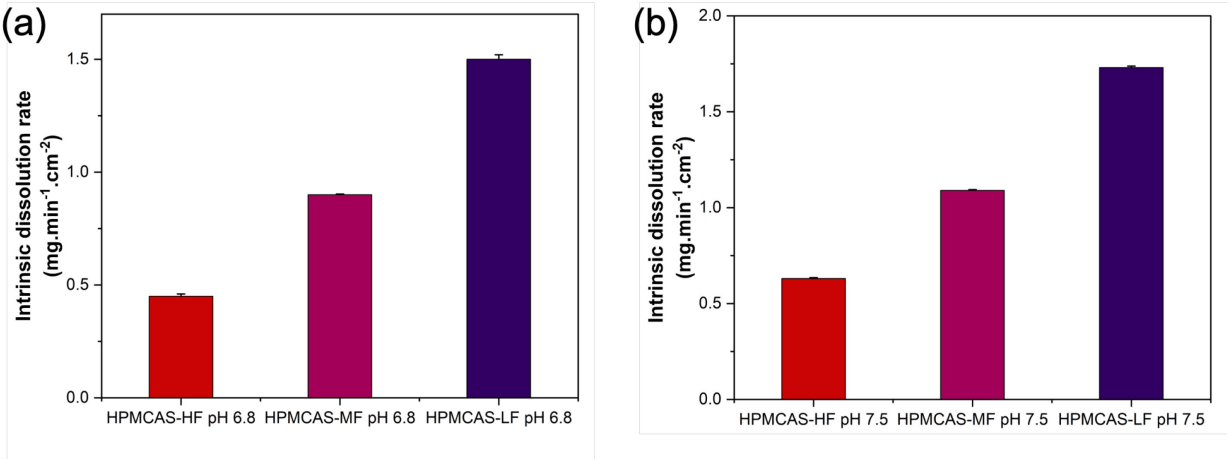

Figure 2. Intrinsic dissolution rates of HF, MF and LF grade of HPMCAS in (a) 50 mM pH 6.8 phosphate buffer, (b) 50 mM pH 7.5 phosphate buffer. Error bars represent standard deviations, n = 3. Release rates of HPMCAS-MF in pH 6.8 and pH 7.5 are taken from Bapat et al.[8]

Figure 3a shows normalized release rates of components from LOR: HPMCAS 25% DL ASDs in 50 mM pH 6.8 phosphate buffer and Figure 3b shows the corresponding normalized release rates at pH 7.5. Drug and polymer released at approximately the same normalized release rate for all systems. The release pattern was similar at both pH conditions with the LOR: HPMCAS-LF ASD showing the highest normalized release rates of both polymer and drug, followed by LOR: HPMCAS-MF and then LOR: HPMCAS-HF ASDs. Comparing between pH conditions, much larger differences in release rates between ASDs prepared with different polymer grades were seen at pH 6.8 versus at pH 7.5. The difference in release rates between HF and LF was a factor of more than 10 at pH 6.8, and less than a factor of 2 at pH 7.5. The release rate from the LOR: HPMCAS-HF ASD was extremely low at pH 6.8 and increased by more than an order of magnitude at pH 7.5. In contrast, the corresponding increases were a factor of ~5 for MF ASDs and a factor of ~3 for ASDs with the LF grade when comparing equivalent grades across the two pH conditions.

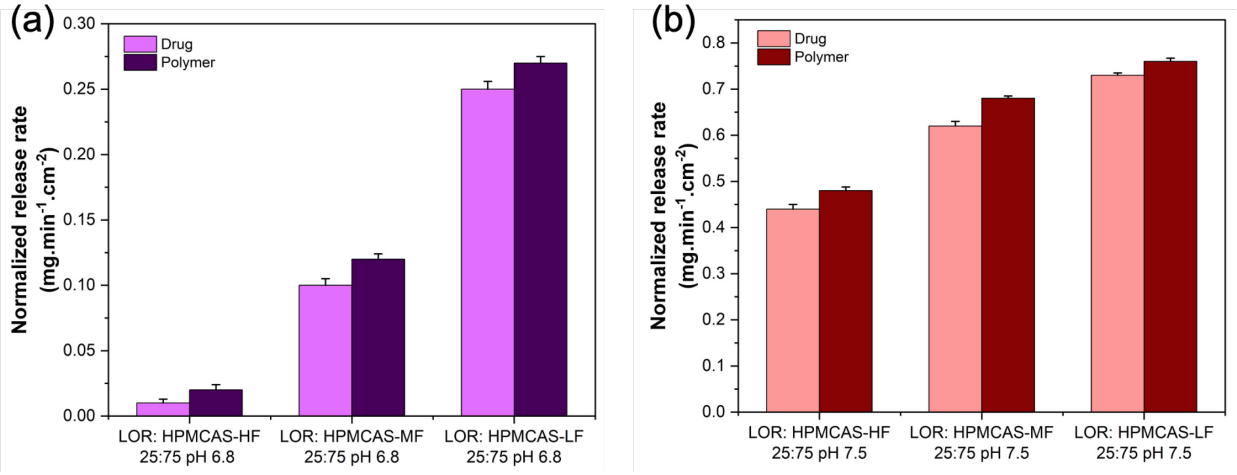

Figure 3. Normalized released rates of LOR: HPMCAS 25:75 w/w ASDs with HF, MF and LF grades of HPMCAS in (a) 50 mM pH 6.8 phosphate buffer, (b) 50 mM pH 7.5 phosphate buffer. Error bars represent standard deviations, n = 3. Normalized release rates of LOR: HPMCAS-MF 25:75 w/w in pH 6.8 and pH 7.5 are taken from Bapat et al.[8]

Figure 4 shows normalized release rates of drug and polymer from CNZ: HPMCAS-MF and CNZ: HPMCAS-LF 25% DL ASDs in 50 mM pH 6.8 phosphate buffer, where it was observed that drug and polymer showed approximately the same normalized release rates. Both components released from the LF ASD with higher normalized release rates when compared to the MF ASD. Release rates increased by a factor of ~ 9 on changing the polymer in the ASD from the MF to the LF grade. The release rate from ASDs prepared with HF was too slow to be determined.

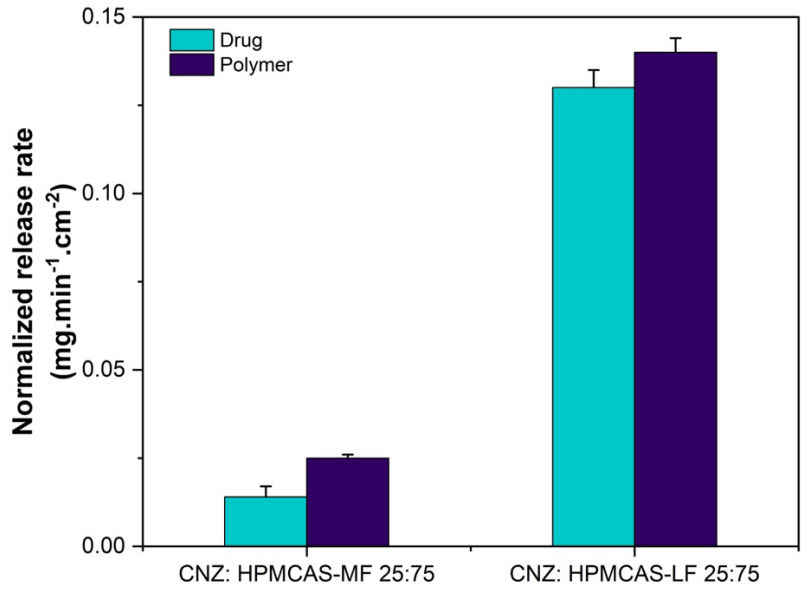

Figure 4. Normalized released rates of CNZ: HPMCAS 25:75 w/w ASDs with MF and LF grades of HPMCAS in 50 mM pH 6.8 phosphate buffer. Error bars represent standard deviations, n = 3. Normalized release rate of CNZ: HPMCAS-MF 25:75 in pH 6.8 is taken from Bapat et al.[8]

A limited set of release experiments was also conducted at low pH conditions and results are summarized in Table S3. Release was less than 5% after 60 min from ASDs of either LOR or CNZ at a 25% DL, regardless of the grade of HPMCAS used. Furthermore, no evidence of drug crystallization was observed over the experimental timeframe.

5.2. Supersaturation Extent of Solutions Generated During Release Experiments

Table 2 summarizes the solution concentrations achieved after 1 h of release for the various dispersions, and also provides information about the amorphous and crystalline solubilities at the relevant pH conditions. No drug crystallization was observed for either drug during the release experiments during the 1 h experimental period, either in solution, or on the surface of the dissolving ASD, which was checked under polarized light microscope at the end of the experiment. Furthermore, no solution or surface crystallization was observed for up to 12 hours following release from ASDs with MF and HF grades with either drug. Some small crystals were observed in the solution after release from the ASD prepared with the LF grade and LOR after about 10 hours. These observations provide assurance that the slow release rates observed for some systems cannot be attributed to crystallization.

Table 2. Solution concentration observed after 1 h of release with corresponding crystalline and amorphous solubility values.

ASD	pH	Solution concentration after 1 hour (μg/mL)	Crystalline solubility of drugs (μg/mL)	Amorphous solubility of drugs (μg/mL)
LOR: HPMCAS-LF	pH 6.8	17.6 ± 0.1	1.8 ± 0.1[3]	9.0 ± 0.1[3]
	pH 7.5	59.1 ± 0.2	1.4 ± 0.1[3]	7.6 ± 0.1[3]
LOR: HPMCAS-MF	pH 6.8	7.0 ± 0.1	1.8 ± 0.1[3]	9.0 ± 0.1[3]
	pH 7.5	39.9 ± 0.0	1.4 ± 0.1[3]	7.6 ± 0.1[3]
LOR: HPMCAS-HF	pH 6.8	2.4 ± 0.1	1.8 ± 0.1[3]	9.0 ± 0.1[3]
	pH 7.5	29.2 ± 0.2	1.4 ± 0.1[3]	7.6 ± 0.1[3]
CNZ: HPMCAS-LF	pH 6.8	5.3 ± 0.2	2.1 ± 0.06[60]	12.0 ± 0.2[61]
CNZ: HPMCAS-MF	pH 6.8	2.7 ± 0.1	2.1 ± 0.06[60]	12.0 ± 0.2[61]
CNZ: HPMCAS-HF	pH 6.8	0.0 ± 0.0	2.1 ± 0.06[60]	12.0 ± 0.2[61]

5.3. Potentiometric Titrations

Figure 5 shows potentiometric titration curves for HPMCAS-LF (Figure 5a) and HPMCAS-HF (Figure 5b) after adding small aliquots of 0.1 N HCl to the dissolved polymer solution. Table 3 summarizes the quantity of -COOH groups and pK_a values calculated using the MATLAB analysis of the potentiometric titration curves.

Table 3. Amount of -COOH groups in polymer and estimated pK_a values. Error bars represents standard deviation n = 2. HPMCAS-MF values were taken from ref[45].

Polymer	Amount of -COOH groups (mmol/g)	**pK_a**
HPMCAS-LF	1.52 ± 0.03	4.91 ± 0.01
HPMCAS-MF	1.19 ± 0.01[45]	4.97 ± 0.02[45]
HPMCAS-HF	0.76 ± 0.02	5.06 ± 0.02

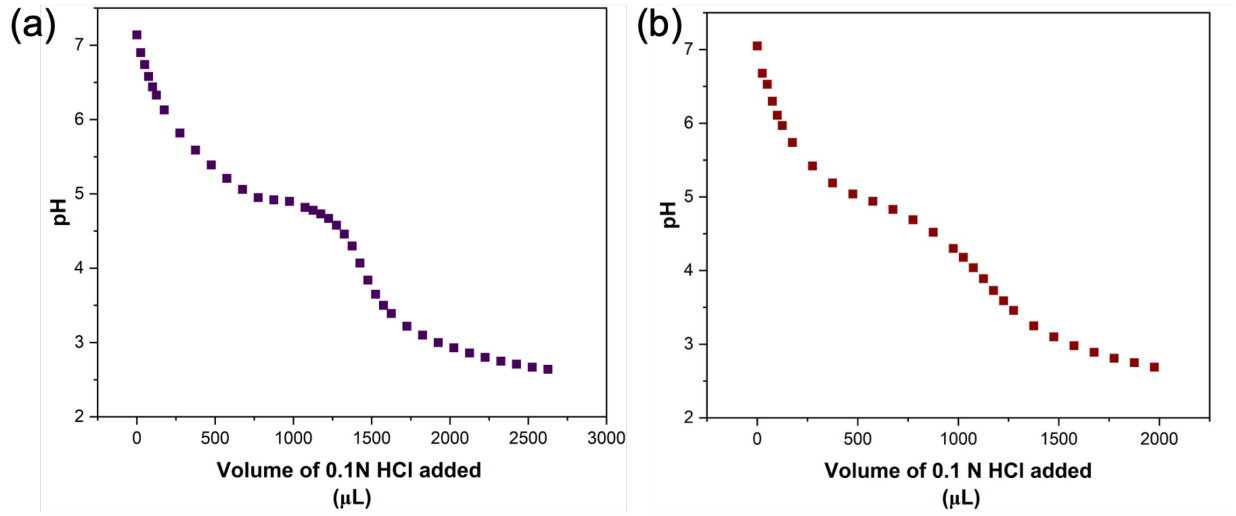

Figure 5. Potentiometric titration curves for (a) HPMCAS-LF, and (b) HPMCAS-HF

5.4. Complexation Experiments

Complexation experiments (Table 4) were performed for CNZ and LOR with different grades of HPMCAS at various molar ratios of drug-to-polymer -COOH groups, as determined from the potentiometric titration curves, at pH 6.0. Figure 6 shows the highest % complexation for HPMCAS-HF with CNZ, followed by HPMCAS-MF while the lowest extent of complexation

was observed for HPMCAS-LF at equivalent molar ratios of CNZ to -COOH polymer groups. Figure 7 shows the complexation extents of the three different grades of polymer with LOR at 1:1 molar ratio of LOR to -COOH polymer groups at various pH conditions. HPMCAS-HF showed higher complexation across the entire pH range studied compared to HPMCAS-MF or HPMCAS-LF. Table 4 summarizes the molar ratio of drug:COOH polymer groups evaluated, their corresponding drug loadings in an ASD and the observed % complexation.

Table 4. Complexation of weakly basic drugs with various grades of HPMCAS at different ratios of drug: COOH groups of the polymer in pH 6.0 phosphate buffer[a]

Drug	Polymer grade	Drug: polymer molar ratio	Corresponding ASD drug loading (%)	Polymer complexation (%)
Cinnarizine (CNZ)	LF	0.25:1	13	30 ± 5
		0.5:1	22	45 ± 3
		0.75:1	30	65 ± 4
		1:1	36	70 ± 6
		1.5:1	46	85 ± 2
		2:1	88	95 ± 3
	HF	0.25:1	7	70 ± 2
		0.5:1	13	86 ± 6
		0.75:1	17	98 ± 4
		1:1	22	99 ± 3
		1.5:1	30	98 ± 4
		2:1	36	98 ± 2
Loratadine (LOR)	LF	1:1	37	50 ± 6
	HF	1:1	22	95 ± 3

[a]Mean values ± standard deviation where n =3.

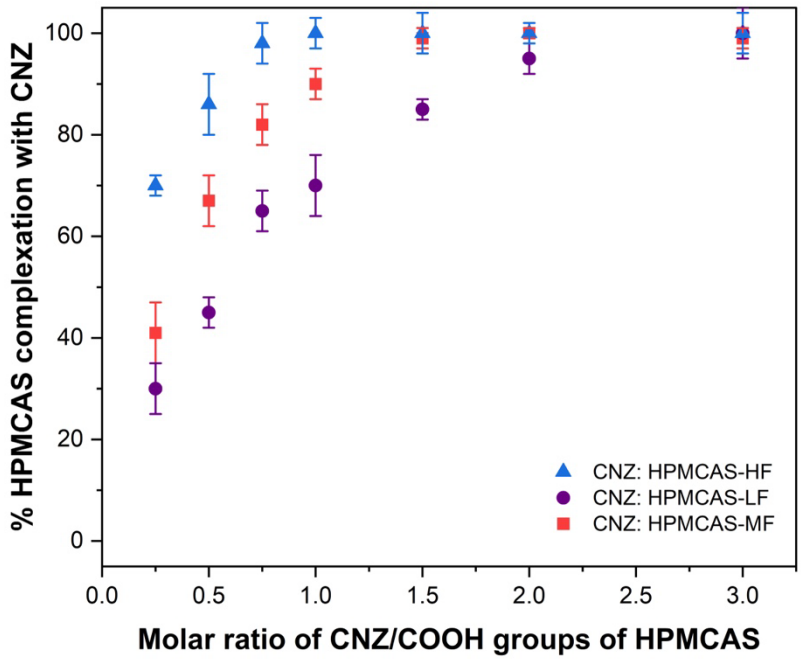

Figure 6. HPMCAS complexation extent at various molar ratios of CNZ to the -COOH groups of HPMCAS-MF, HPMCAS-LF and HPMCAS-HF in pH 6.0 phosphate buffer. Error bars represent standard deviations, n = 3. HPMCAS-MF data taken from Bapat et al.[3]

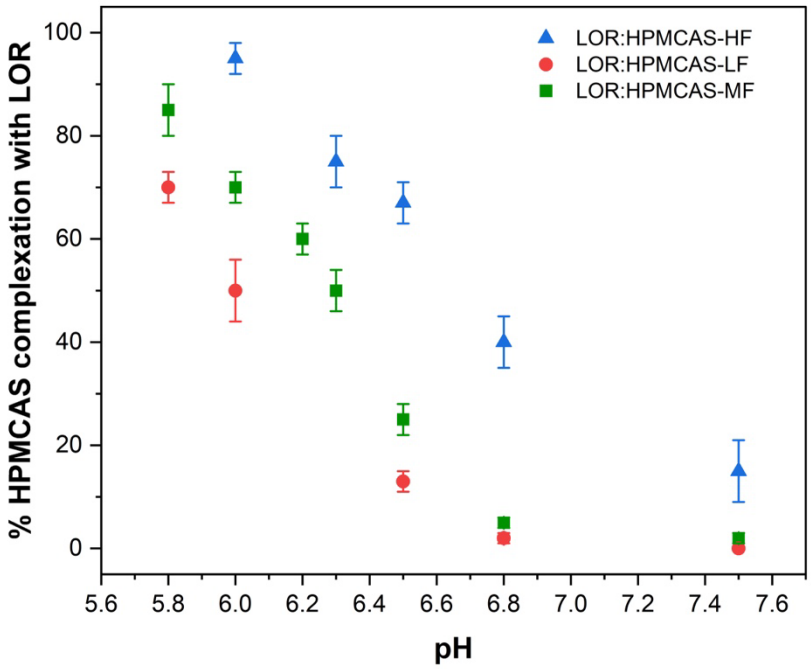

Figure 7. HPMCAS complexation with LOR in solutions of different pH at a 1:1 molar ratio of LOR to -COOH groups of HPMCAS-MF, HPMCAS-LF and HPMCAS-HF. Error bars represent standard deviations, n = 3. HPMCAS-MF data taken from Bapat et al.[3]

Complexation between LF or MF and CNZ was also evaluated at a slightly lower pH of 5.8 where the polymer ionization extent is somewhat reduced while still maintaining solubility, and the drug is still fully ionized. At pH 5.8, based on a pKa value of 4.9, HPMCAS is expected to be 89% ionized. Results are summarized in Figure 8 where the extent of complexation is compared to results obtained at pH 6.0. It is apparent that when the drug is fully ionized, the extent of complexation is increased by a decrease in the polymer ionization extent. This is because the polymer solubility is reduced as the extent of polymer ionization is decreased, while the ratio of positively charged drug groups to negatively charged polymer groups is increased slightly.

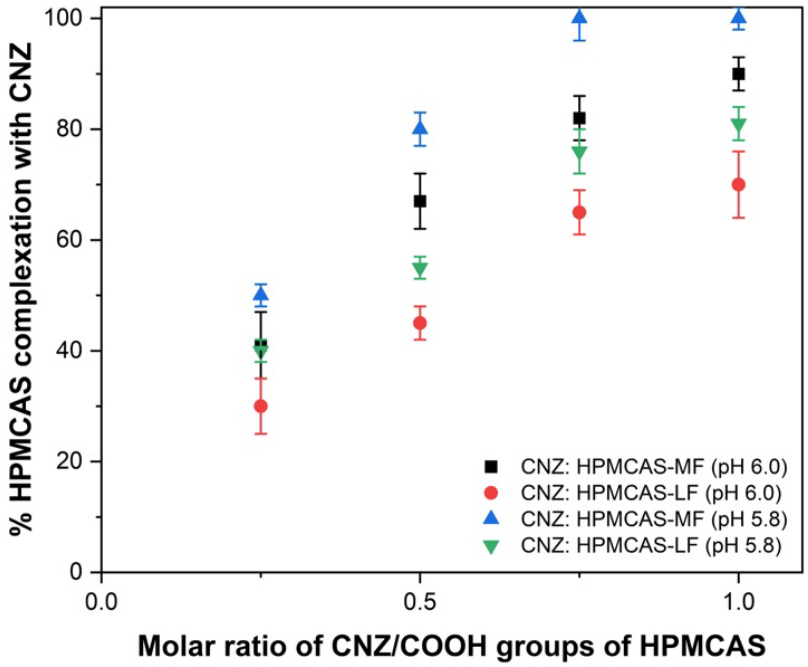

Figure 8. Comparison of complexation extent between HPMCAS LF or MF grades and CNZ at pH 5.8 and 6.0. Error bars represent standard deviations, n = 3. HPMCAS-MF data at pH 6.0 taken from Bapat et al.[3]

5.5. Equilibrium Surface pH Measurement

Table 5 represents the final equilibrated pH value for each polymer grade of HPMCAS in a saturated solution where this value is taken as the surface pH of undissolved polymer particles in

water. HPMCAS-LF is the most acidic with the lowest surface pH whereas HPMCAS-HF had the highest surface pH value, reflecting their different solubilities.

Table 5. Equilibrium surface pH of neat HPMCAS polymer grades

Polymer Grade	Surface pH
HPMCAS-LF	4.52 ± 0.04
HPMCAS-MF	4.61 ± 0.02
HPMCAS-HF	4.73 ± 0.03

6. Discussion

Ionic interactions between drugs and polymers have attracted interest for a variety of applications.[62–68] In the context of amorphous solid dispersions there have been several studies of proton transfer from a weakly basic drug to an acidic polymer in the solid ASD after preparation. Weuts et al. reported the formation of ionic interactions between polyacrylic acid and loperamide as well as loperamide derivatives. Based on extensive characterization, they reported a number of potential advantages arising from the interactions, namely an enhanced ASD glass transition temperature, improved storage stability against crystallization and rapid drug release.[69] This initial study has spurred several additional investigations, spanning different drugs and polymers. In particular, solid state interactions between lumefantrine and acidic polymers have been widely studied by several groups.[48,70,71] Other drugs where ionic interactions with acidic polymers have been reported in the solid ASD include ciprofloxacin,[72] clofazamine,[73] gefitinib,[48] lapatanib,[74] and ketonconazole.[75]

In terms of in vitro delivery performance, it was reported that release of the lipophilic drugs, lumefantrine and clozapine was enhanced through salt formation with polyacrylic acid.[76] In contrast, lumefantrine demonstrated a reduction in release rate from ASDs with enteric polymers as a function of drug loading, while release was rapid when formulated with a neutral polymer.[45]

The conflict between the release results observed for lumefantrine ASDs formulated with polyacrylic acid versus enteric polymers may be related to the overall hydrophilicity of the polymer. Polyacrylic acid is soluble across all pH conditions, even when un-ionized. In contrast, enteric polymers only become soluble once a critical ionization extent is reached at which the polymer strands become sufficiently hydrated to dissolve and release from the matrix. Therefore, components molecularly mixed with the polymer that can impede hydration of a critical number of ionizable groups are likely to be detrimental for release. This was studied in depth in a recent study with HPMCAS-MF ASDs with a number of different lipophilic drugs.[3] pH conditions leading to mutual ionization of lipophilic weak base drugs and HPMCAS-MF led to reduced release rates of components from the ASD, and increased formation of insoluble drug-polymer complexes.

The popularity of HPMCAS as an ASD polymer,[77] as well as the increasing interest in formulating drug-polymer salts to enhance drug stability against crystallization warrants additional investigations of the impact of drug-polymer ionic interactions on release performance, extending previous work to consider different HPMCAS grades. Ideally, the improved physical stability to crystallization resulting from salt formation in the ASD can be balanced with the reduced release extent observed for pH conditions where mutual ionization persists. For the three grades of HPMCAS studied herein, we found that the LF grade shows improved release performance when formulated with model weak base lipophilic drugs, relative to the MF and HF grades (Figures 3 and 4), for a pH where both components are ionized. Neat LF also has a faster dissolution rate than the other HPMCAS grades at pH 6.8 (Figure 2). To rationalize these observations, we can utilize observations made by Heller and coworkers in their extensive study of partial esters of vinyl acetate-maleic anhydride polymers.[78] These are

hydrophobic polymers that are solubilized by ionization of carboxylic acid groups. The authors described these polymers as containing two components, a hydrophobic moiety, and a solubilizing group, namely the COOH group. They observed that when the hydrophobic moiety became larger, a larger extent of ionization was required to solubilize the polymer, corresponding to a higher dissolution pH (pK_a remained unchanged with a change in hydrophobic group size). Thus, when the ester contained a C_2H_5 group, only 3% of carboxyl ionization was required for polymer solubilization, whereas the critical extent of ionization increased to 91% for a C_9H_{19} group. A similar explanation can be applied to the different grades of HPMCAS, where pK_a values are minimally different between the grades (Table 3). LF has a larger ratio of hydrophilic (succinoyl) to hydrophobic (acetate) groups, and consequently requires a lower degree of ionization to solubilize, and hence has a lower dissolution pH threshold than the other grades. In addition, as shown in Table 3, LF has more ionizable groups per polymer chain than the other grades, twice the number per gram of polymer as the HF grade. Therefore, it is fairly straightforward to rationalize the lower relative impact of the drug on release rates from the ASD formulated with the LF grade versus the HF grade at a given weight fraction of drug. The LF grade is both more soluble at pH 6.8 than the HF grade as it has less hydrophobic groups, and for a given amount of drug in the ASD (25% DL), it has more carboxylate groups (twice as many as the HF grade, Table 3), allowing "spare" carboxylate groups (i.e. those not involved in electrostatic interactions with the cationic drug) to contribute to hydration. The higher solubility of the LF grade is reflected by the complexation experiments, where the molar ratio of drug:COOH groups of the polymer was kept constant (Figure 6). At a 1:1 ratio, nearly 100% of HF forms an insoluble complex with CNZ, while only ~70% of LF is precipitated, suggesting that the latter grade is more soluble in the presence of the drug, at a given stoichiometric ratio.

Similar trends were observed for LOR, although the extent of complexation for LF at pH 6.0 was lower than in the case of CNZ (Figure 7). pH 6.0 is a relevant condition to study complex formation, as this is the pH at the dissolving ASD surface for a bulk solution pH of 6.8 (and with 50 mM phosphate buffer).[8] Polymer solubility at the interface impacts the polymer diffusion rate across the aqueous boundary layer into the bulk aqueous solution, and in turn, the dissolution rate. Given that the drug release is coupled to polymer dissolution, as evidenced by the similar normalized release rates of the two components, the impact of drug-polymer complexation on release rates can be rationalized. This can be exemplified by comparing the release rates of the 25% DL ASDs at a bulk solution pH of 6.8 with CNZ versus LOR (Figures 3 and 4). For LF, the release rate of components from the LOR ASD is higher than from the corresponding CNZ ASD, even though the molar ratios of the drug: polymer COOH group are similar. Based on Log P values, both drugs are lipophilic; Log P of 5.8 for CNZ and 5.2 for LOR. Thus, the difference in release rates can be most likely attributed to the lower extent of complexation of LOR with LF at pH 6.0 rather than lipophilicity differences. For example, comparing the complexation extent at a 1:1 molar ratio from Figures 6 and 7 reveals values of approximately 70% for CNZ and 50% for LOR, at pH 6.0. Thus, HPMCAS-LF is more soluble in the presence of LOR than CNZ, and the release rate of polymer and drug from the ASD is correspondingly higher. In turn, this difference in interaction tendency between LF and CNZ versus LOR can be accounted for, at least partially, based on the ionization extent of the two drugs at the ASD surface pH of 6.0; CNZ with a pK_a of 8.4[79] is essentially completely ionized (>99.9% ionized at pH 6.0), whereas LOR with a pK_a of 5.2[80] is only partially ionized (~14% ionized at pH 6.0). The importance of ionization is illustrated in Figure 7, which shows that the extent of drug-polymer insoluble complex formation

falls off steeply with an increase in pH as LOR ionization extent is reduced (Figure S1), a trend seen for all three polymer grades.

7. Conclusions

Release rates of two cationic drugs from ASDs with HPMCAS were found to vary with polymer grade as well as with the extent of ionization of the drug. The higher dissolution rate of HPMCAS-LF translated to improved drug release from the ASD relative to ASDs formulated with HPMCAS-MF or HF. However, the release from the ASD was compromised by drug: polymer electrostatic interactions leading to the formation of an insoluble complex, which in turn reduced the release rates of drug and polymer. The extent of insoluble complex formation was more extensive for HPMCAS-HF versus HPMCAS-LF at any particular drug: polymer COOH molar ratio. The extent of insoluble complex formation, and consequently the release rate of the ASD components, was also impacted by the extent of drug ionization, and hence the pH of the release medium. These observations highlight the convoluted release behavior from ASDs with an acidic polymer and a basic drug and provide a baseline for understanding release properties under more physiologically relevant conditions. Additional studies are needed to evaluate the impact of solubilizing components such as those found in biorelevant simulated intestinal fluids on drug: polymer complex formation.

8. Acknowledgements

The support of Ross-Lynn Research Scholar Award 2023-24 from Purdue University College of Pharmacy is gratefully acknowledged. The National Science Foundation is acknowledged for funding (DMR- 2204995).

ASSOCIATED CONTENT

Supporting Information

Ionization of loratadine as a function of pH compared to complexation extent. Composition of various phosphate buffer solutions, HPLC gradient quantification method for HPMCAS

9. References

(1) Beig, A.; Fine-Shamir, N.; Lindley, D.; Miller, J. M.; Dahan, A. Advantageous Solubility-Permeability Interplay When Using Amorphous Solid Dispersion (ASD) Formulation for the BCS Class IV P-Gp Substrate Rifaximin: Simultaneous Increase of Both the Solubility and the Permeability. *AAPS J* **2017**, *19* (3), 806–813. https://doi.org/10.1208/s12248-017-0052-1.

(2) Niessen, J.; López Mármol, Á.; Ismail, R.; Schiele, J. T.; Rau, K.; Wahl, A.; Sauer, K.; Heinzerling, O.; Breitkreutz, J.; Koziolek, M. Application of Biorelevant in Vitro Assays for the Assessment and Optimization of ASD-Based Formulations for Pediatric Patients. *European Journal of Pharmaceutics and Biopharmaceutics* **2023**, *185*, 13–27. https://doi.org/10.1016/j.ejpb.2023.02.008.

(3) Bapat, P.; Paul, S.; Tseng, Y.-C.; Taylor, L. S. Interplay of Drug–Polymer Interactions and Release Performance for HPMCAS-Based Amorphous Solid Dispersions. *Mol. Pharmaceutics* **2024**, *21* (3), 1466–1478. https://doi.org/10.1021/acs.molpharmaceut.3c01106.

(4) Bhujbal, S. V.; Mitra, B.; Jain, U.; Gong, Y.; Agrawal, A.; Karki, S.; Taylor, L. S.; Kumar, S.; (Tony) Zhou, Q. Pharmaceutical Amorphous Solid Dispersion: A Review of Manufacturing Strategies. *Acta Pharmaceutica Sinica B* **2021**, *11* (8), 2505–2536. https://doi.org/10.1016/j.apsb.2021.05.014.

(5) Frank, D. S.; Punia, A.; Fahy, M.; Dalton, C.; Rowe, J.; Schenck, L. Densifying Co-Precipitated Amorphous Dispersions to Achieve Improved Bulk Powder Properties. *Pharm Res* **2022**, *39* (12), 3197–3208. https://doi.org/10.1007/s11095-022-03416-6.

(6) Vodak, D. T.; Morgen, M. Design and Development of HPMCAS-Based Spray-Dried Dispersions. In *Amorphous Solid Dispersions: Theory and Practice*; Shah, N., Sandhu, H., Choi, D. S., Chokshi, H., Malick, A. W., Eds.; Advances in Delivery Science and Technology; Springer: New York, NY, 2014; pp 303–322. https://doi.org/10.1007/978-1-4939-1598-9_9.

(7) Li, B.; Konecke, S.; Wegiel, L. A.; Taylor, L. S.; Edgar, K. J. Both Solubility and Chemical Stability of Curcumin Are Enhanced by Solid Dispersion in Cellulose Derivative Matrices. *Carbohydrate Polymers* **2013**, *98* (1), 1108–1116. https://doi.org/10.1016/j.carbpol.2013.07.017.

(8) Bapat, P.; Paul, S.; Thakral, N. K.; Tseng, Y.-C.; Taylor, L. S. Does Media Choice Matter When Evaluating the Performance of Hydroxypropyl Methylcellulose Acetate Succinate-Based Amorphous Solid Dispersions? *Mol. Pharmaceutics* **2023**. https://doi.org/10.1021/acs.molpharmaceut.3c00586.

(9) Hancock, B. C.; Zografi, G. The Relationship Between the Glass Transition Temperature and the Water Content of Amorphous Pharmaceutical Solids. *Pharm Res* **1994**, *11* (4), 471–477. https://doi.org/10.1023/A:1018941810744.
(10) Hancock, B. C.; Parks, M. What Is the True Solubility Advantage for Amorphous Pharmaceuticals? *Pharm Res* **2000**, *17* (4), 397–404. https://doi.org/10.1023/A:1007516718048.
(11) Frank, D. S.; Prasad, P.; Iuzzolino, L.; Schenck, L. Dissolution Behavior of Weakly Basic Pharmaceuticals from Amorphous Dispersions Stabilized by a Poly(Dimethylaminoethyl Methacrylate) Copolymer. *Mol. Pharmaceutics* **2022**, *19* (9), 3304–3313. https://doi.org/10.1021/acs.molpharmaceut.2c00456.
(12) Cheow, W. S.; Hadinoto, K. Self-Assembled Amorphous Drug–Polyelectrolyte Nanoparticle Complex with Enhanced Dissolution Rate and Saturation Solubility. *Journal of Colloid and Interface Science* **2012**, *367* (1), 518–526. https://doi.org/10.1016/j.jcis.2011.10.011.
(13) Ueda, K.; Hate, S. S.; Taylor, L. S. Impact of Hypromellose Acetate Succinate Grade on Drug Amorphous Solubility and In Vitro Membrane Transport. *Journal of Pharmaceutical Sciences* **2020**, *109* (8), 2464–2473. https://doi.org/10.1016/j.xphs.2020.04.014.
(14) Ueda, K.; Higashi, K.; Moribe, K. Mechanistic Elucidation of Formation of Drug-Rich Amorphous Nanodroplets by Dissolution of the Solid Dispersion Formulation. *International Journal of Pharmaceutics* **2019**, *561*, 82–92. https://doi.org/10.1016/j.ijpharm.2019.02.034.
(15) Indulkar, A. S.; Lou, X.; Zhang, G. G. Z.; Taylor, L. S. Insights into the Dissolution Mechanism of Ritonavir–Copovidone Amorphous Solid Dispersions: Importance of Congruent Release for Enhanced Performance. *Mol. Pharmaceutics* **2019**, *16* (3), 1327–1339. https://doi.org/10.1021/acs.molpharmaceut.8b01261.
(16) Que, C.; Lou, X.; Zemlyanov, D. Y.; Mo, H.; Indulkar, A. S.; Gao, Y.; Zhang, G. G. Z.; Taylor, L. S. Insights into the Dissolution Behavior of Ledipasvir–Copovidone Amorphous Solid Dispersions: Role of Drug Loading and Intermolecular Interactions. *Mol. Pharmaceutics* **2019**, *16* (12), 5054–5067. https://doi.org/10.1021/acs.molpharmaceut.9b01025.
(17) Que, C.; Deac, A.; Zemlyanov, D. Y.; Qi, Q.; Indulkar, A. S.; Gao, Y.; Zhang, G. G. Z.; Taylor, L. S. Impact of Drug–Polymer Intermolecular Interactions on Dissolution Performance of Copovidone-Based Amorphous Solid Dispersions. *Mol. Pharmaceutics* **2021**, *18* (9), 3496–3508. https://doi.org/10.1021/acs.molpharmaceut.1c00419.
(18) Liu, L.; Chen, L.; Müllers, W.; Serno, P.; Qian, F. Water-Resistant Drug–Polymer Interaction Contributes to the Formation of Nano-Species during the Dissolution of Felodipine Amorphous Solid Dispersions. *Mol. Pharmaceutics* **2022**, *19* (8), 2888–2899. https://doi.org/10.1021/acs.molpharmaceut.2c00250.
(19) Kothari, K.; Ragoonanan, V.; Suryanarayanan, R. The Role of Drug–Polymer Hydrogen Bonding Interactions on the Molecular Mobility and Physical Stability of Nifedipine Solid Dispersions. *Mol. Pharmaceutics* **2015**, *12* (1), 162–170. https://doi.org/10.1021/mp5005146.
(20) Khougaz, K.; Clas, S. Crystallization Inhibition in Solid Dispersions of MK-0591 and Poly(Vinylpyrrolidone) Polymers. *Journal of Pharmaceutical Sciences* **2000**, *89* (10), 1325–1334. https://doi.org/10.1002/1520-6017(200010)89:10<1325::AID-JPS10>3.0.CO;2-5.

(21) Berger, G.; Soubhye, J.; Meyer, F. Halogen Bonding in Polymer Science: From Crystal Engineering to Functional Supramolecular Polymers and Materials. *Polymer Chemistry* **2015**, *6* (19), 3559–3580. https://doi.org/10.1039/C5PY00354G.
(22) Asmussen, F.; Ueberreiter, K. Velocity of Dissolution of Polymers. Part II. *Journal of Polymer Science* **1962**, *57* (165), 199–208. https://doi.org/10.1002/pol.1962.1205716516.
(23) Alvarenga, B. R. de Jr.; Moseson, D. E.; Carneiro, R. L.; Taylor, L. S. Impact of Polymer Type on Thermal Degradation of Amorphous Solid Dispersions Containing Ritonavir. *Mol. Pharmaceutics* **2022**, *19* (1), 332–344. https://doi.org/10.1021/acs.molpharmaceut.1c00823.
(24) Chen, Y.; Wang, S.; Wang, S.; Liu, C.; Su, C.; Hageman, M.; Hussain, M.; Haskell, R.; Stefanski, K.; Qian, F. Initial Drug Dissolution from Amorphous Solid Dispersions Controlled by Polymer Dissolution and Drug-Polymer Interaction. *Pharm Res* **2016**, *33* (10), 2445–2458. https://doi.org/10.1007/s11095-016-1969-2.
(25) Chen, Y.; Liu, C.; Chen, Z.; Su, C.; Hageman, M.; Hussain, M.; Haskell, R.; Stefanski, K.; Qian, F. Drug–Polymer–Water Interaction and Its Implication for the Dissolution Performance of Amorphous Solid Dispersions. *Mol. Pharmaceutics* **2015**, *12* (2), 576–589. https://doi.org/10.1021/mp500660m.
(26) Saboo, S.; Kestur, U. S.; Flaherty, D. P.; Taylor, L. S. Congruent Release of Drug and Polymer from Amorphous Solid Dispersions: Insights into the Role of Drug-Polymer Hydrogen Bonding, Surface Crystallization, and Glass Transition. *Mol. Pharmaceutics* **2020**, *17* (4), 1261–1275. https://doi.org/10.1021/acs.molpharmaceut.9b01272.
(27) Saboo, S.; Mugheirbi, N. A.; Zemlyanov, D. Y.; Kestur, U. S.; Taylor, L. S. Congruent Release of Drug and Polymer: A "Sweet Spot" in the Dissolution of Amorphous Solid Dispersions. *Journal of Controlled Release* **2019**, *298*, 68–82. https://doi.org/10.1016/j.jconrel.2019.01.039.
(28) Saboo, S.; Bapat, P.; Moseson, D. E.; Kestur, U. S.; Taylor, L. S. Exploring the Role of Surfactants in Enhancing Drug Release from Amorphous Solid Dispersions at Higher Drug Loadings. *Pharmaceutics* **2021**, *13* (5), 735. https://doi.org/10.3390/pharmaceutics13050735.
(29) Deac, A.; Qi, Q.; Indulkar, A. S.; Purohit, H. S.; Gao, Y.; Zhang, G. G. Z.; Taylor, L. S. Dissolution Mechanisms of Amorphous Solid Dispersions: Role of Drug Load and Molecular Interactions. *Mol. Pharmaceutics* **2023**, *20* (1), 722–737. https://doi.org/10.1021/acs.molpharmaceut.2c00892.
(30) Purohit, H. S.; Taylor, L. S. Phase Behavior of Ritonavir Amorphous Solid Dispersions during Hydration and Dissolution. *Pharm Res* **2017**, *34* (12), 2842–2861. https://doi.org/10.1007/s11095-017-2265-5.
(31) Purohit, H. S.; Ormes, J. D.; Saboo, S.; Su, Y.; Lamm, M. S.; Mann, A. K. P.; Taylor, L. S. Insights into Nano- and Micron-Scale Phase Separation in Amorphous Solid Dispersions Using Fluorescence-Based Techniques in Combination with Solid State Nuclear Magnetic Resonance Spectroscopy. *Pharm Res* **2017**, *34* (7), 1364–1377. https://doi.org/10.1007/s11095-017-2145-z.
(32) Yang, R.; Zhang, G. G. Z.; Zemlyanov, D. Y.; Purohit, H. S.; Taylor, L. S. Release Mechanisms of Amorphous Solid Dispersions: Role of Drug-Polymer Phase Separation and Morphology. *Journal of Pharmaceutical Sciences* **2023**, *112* (1), 304–317. https://doi.org/10.1016/j.xphs.2022.10.021.

(33) Simonelli, A. P.; Mehta, S. C.; Higuchi, W. I. Dissolution Rates of High Energy Polyvinylpyrrolidone (PVP)-Sulfathiazole Coprecipitates. *Journal of Pharmaceutical Sciences* **1969**, *58* (5), 538–549. https://doi.org/10.1002/jps.2600580503.
(34) Simonelli, A. P.; Meshali, M. M.; El-Gawad, A. H. A.; Abdel-Aleem, H. M.; Gabr, K. E. Effect of Some Polymers on the Physico-Chemical and Dissolution Properties of Hydrochlorothiazide II. *Drug Development and Industrial Pharmacy* **1994**, *20* (17), 2741–2752. https://doi.org/10.3109/03639049409042677.
(35) Indulkar, A. S.; Waters, J. E.; Mo, H.; Gao, Y.; Raina, S. A.; Zhang, G. G. Z.; Taylor, L. S. Origin of Nanodroplet Formation Upon Dissolution of an Amorphous Solid Dispersion: A Mechanistic Isotope Scrambling Study. *Journal of Pharmaceutical Sciences* **2017**, *106* (8), 1998–2008. https://doi.org/10.1016/j.xphs.2017.04.015.
(36) Chailu Que; Qi, Q.; Zemlyanov, D. Y.; Mo, H.; Deac, A.; Zeller, M.; Indulkar, A. S.; Gao, Y.; Zhang, G. G. Z.; Taylor, L. S. Evidence for Halogen Bonding in Amorphous Solid Dispersions. *Crystal Growth & Design* **2020**, *20* (5), 3224–3235. https://doi.org/10.1021/acs.cgd.0c00073.
(37) Curatolo, W.; Nightingale, J. A.; Herbig, S. M. Utility of Hydroxypropylmethylcellulose Acetate Succinate (HPMCAS) for Initiation and Maintenance of Drug Supersaturation in the GI Milieu. *Pharm Res* **2009**, *26* (6), 1419–1431. https://doi.org/10.1007/s11095-009-9852-z.
(38) Liu, J.; Li, Y.; Ao, W.; Xiao, Y.; Bai, M.; Li, S. Preparation and Characterization of Aprepitant Solid Dispersion with HPMCAS-LF. *ACS Omega* **2022**, *7* (44), 39907–39912. https://doi.org/10.1021/acsomega.2c04021.
(39) Zhang, Q.; Zhao, Y.; Zhao, Y.; Ding, Z.; Fan, Z.; Zhang, H.; Liu, M.; Wang, Z.; Han, J. Effect of HPMCAS on Recrystallization Inhibition of Nimodipine Solid Dispersions Prepared by Hot-Melt Extrusion and Dissolution Enhancement of Nimodipine Tablets. *Colloids and Surfaces B: Biointerfaces* **2018**, *172*, 118–126. https://doi.org/10.1016/j.colsurfb.2018.08.030.
(40) Tanno, F.; Nishiyama, Y.; Kokubo, H.; Obara, S. Evaluation of Hypromellose Acetate Succinate (HPMCAS) as a Carrier in Solid Dispersions. *Drug Development and Industrial Pharmacy* **2004**, *30* (1), 9–17. https://doi.org/10.1081/DDC-120027506.
(41) Stewart, A. M.; Grass, M. E.; Brodeur, T. J.; Goodwin, A. K.; Morgen, M. M.; Friesen, D. T.; Vodak, D. T. Impact of Drug-Rich Colloids of Itraconazole and HPMCAS on Membrane Flux in Vitro and Oral Bioavailability in Rats. *Mol. Pharmaceutics* **2017**, *14* (7), 2437–2449. https://doi.org/10.1021/acs.molpharmaceut.7b00338.
(42) Corrigan, O. I. Mechanisms of Dissolution of Fast Release Solid Dispersions. *Drug Development and Industrial Pharmacy* **1985**, *11* (2–3), 697–724. https://doi.org/10.3109/03639048509056896.
(43) Nguyen, H. T.; Van Duong, T.; Taylor, L. S. Impact of Gastric pH Variations on the Release of Amorphous Solid Dispersion Formulations Containing a Weakly Basic Drug and Enteric Polymers. *Mol. Pharmaceutics* **2023**, *20* (3), 1681–1695. https://doi.org/10.1021/acs.molpharmaceut.2c00895.
(44) Nguyen, H. T.; Van Duong, T.; Jaw-Tsai, S.; Bruning-Barry, R.; Pande, P.; Taneja, R.; Taylor, L. S. Fed- and Fasted-State Performance of Pretomanid Amorphous Solid Dispersions Formulated with an Enteric Polymer. *Mol Pharm* **2023**, *20* (6), 3170–3186. https://doi.org/10.1021/acs.molpharmaceut.3c00174.

(45) Hiew, T. N.; Zemlyanov, D. Y.; Taylor, L. S. Balancing Solid-State Stability and Dissolution Performance of Lumefantrine Amorphous Solid Dispersions: The Role of Polymer Choice and Drug–Polymer Interactions. *Mol. Pharmaceutics* **2022**, *19* (2), 392–413. https://doi.org/10.1021/acs.molpharmaceut.1c00481.
(46) Tsiartas, P. C.; Flanagin, L. W.; Henderson, C. L.; Hinsberg, W. D.; Sanchez, I. C.; Bonnecaze, R. T.; Willson, C. G. The Mechanism of Phenolic Polymer Dissolution: A New Perspective. *Macromolecules* **1997**, *30* (16), 4656–4664. https://doi.org/10.1021/ma9707594.
(47) Chen, Y.; Wang, S.; Wang, S.; Liu, C.; Su, C.; Hageman, M.; Hussain, M.; Haskell, R.; Stefanski, K.; Qian, F. Sodium Lauryl Sulfate Competitively Interacts with HPMC-AS and Consequently Reduces Oral Bioavailability of Posaconazole/HPMC-AS Amorphous Solid Dispersion. *Mol. Pharmaceutics* **2016**, *13* (8), 2787–2795. https://doi.org/10.1021/acs.molpharmaceut.6b00391.
(48) Song, Y.; Zemlyanov, D.; Chen, X.; Su, Z.; Nie, H.; Lubach, J. W.; Smith, D.; Byrn, S.; Pinal, R. Acid-Base Interactions in Amorphous Solid Dispersions of Lumefantrine Prepared by Spray-Drying and Hot-Melt Extrusion Using X-Ray Photoelectron Spectroscopy. *International Journal of Pharmaceutics* **2016**, *514* (2), 456–464. https://doi.org/10.1016/j.ijpharm.2016.06.126.
(49) Nunes, P. D.; Pinto, J. F.; Henriques, J.; Paiva, A. M. Insights into the Release Mechanisms of ITZ:HPMCAS Amorphous Solid Dispersions: The Role of Drug-Rich Colloids. *Mol. Pharmaceutics* **2022**, *19* (1), 51–66. https://doi.org/10.1021/acs.molpharmaceut.1c00578.
(50) Ueda, K.; Higashi, K.; Yamamoto, K.; Moribe, K. The Effect of HPMCAS Functional Groups on Drug Crystallization from the Supersaturated State and Dissolution Improvement. *International Journal of Pharmaceutics* **2014**, *464* (1), 205–213. https://doi.org/10.1016/j.ijpharm.2014.01.005.
(51) Rumondor, A. C. F.; Taylor, L. S. Effect of Polymer Hygroscopicity on the Phase Behavior of Amorphous Solid Dispersions in the Presence of Moisture. *Mol. Pharmaceutics* **2010**, *7* (2), 477–490. https://doi.org/10.1021/mp9002283.
(52) Rumondor, A. C. F.; Stanford, L. A.; Taylor, L. S. Effects of Polymer Type and Storage Relative Humidity on the Kinetics of Felodipine Crystallization from Amorphous Solid Dispersions. *Pharm Res* **2009**, *26* (12), 2599–2606. https://doi.org/10.1007/s11095-009-9974-3.
(53) Al-Gousous, J.; Ruan, H.; Blechar, J. A.; Sun, K. X.; Salehi, N.; Langguth, P.; Job, N. M.; Lipka, E.; Loebenberg, R.; Bermejo, M.; Amidon, G. E.; Amidon, G. L. Mechanistic Analysis and Experimental Verification of Bicarbonate-Controlled Enteric Coat Dissolution: Potential in Vivo Implications. *European Journal of Pharmaceutics and Biopharmaceutics* **2019**, *139*, 47–58. https://doi.org/10.1016/j.ejpb.2019.03.012.
(54) Li, N.; Ormes, J. D.; Taylor, L. S. Leaching of Lopinavir Amorphous Solid Dispersions in Acidic Media. *Pharm Res* **2016**, *33* (7), 1723–1735. https://doi.org/10.1007/s11095-016-1913-5.
(55) Wang, S.; Liu, C.; Chen, Y.; Zhang, Z.; Zhu, A.; Qian, F. A High-Sensitivity HPLC-ELSD Method for HPMC-AS Quantification and Its Application in Elucidating the Release Mechanism of HPMC-AS Based Amorphous Solid Dispersions. *European Journal of Pharmaceutical Sciences* **2018**, *122*, 303–310. https://doi.org/10.1016/j.ejps.2018.07.007.
(56) *Shin-Etsu AQOAT® for amorphous solid dispersion - SE Tylose*. https://www.setylose.com/en/products/healthcare/shinetsu-aqoat (accessed 2024-04-30).

(57) *Shin-Etsu AQOAT® | For Pharmaceutical | Shin-Etsu*. https://www.metolose.jp/en/pharmaceutical/aqoat.html (accessed 2024-04-30).
(58) Fukasawa, M.; Obara, S. Molecular Weight Determination of Hypromellose Acetate Succinate (HPMCAS) Using Size Exclusion Chromatography with a Multi-Angle Laser Light Scattering Detector. *Chemical and Pharmaceutical Bulletin* **2004**, *52* (11), 1391–1393. https://doi.org/10.1248/cpb.52.1391.
(59) Pudipeddi, M.; Zannou, E. A.; Vasanthavada, M.; Dontabhaktuni, A.; Royce, A. E.; Joshi, Y. M.; Serajuddin, A. T. M. Measurement of Surface pH of Pharmaceutical Solids: A Critical Evaluation of Indicator Dye-Sorption Method and Its Comparison With Slurry pH Method. *Journal of Pharmaceutical Sciences* **2008**, *97* (5), 1831–1842. https://doi.org/10.1002/jps.21052.
(60) Maghsoodi, M.; Astemal, S. M.; Nokhodchi, A.; Kiaie, H.; Khoshfetrat, A. B.; Talebi, F. An Insight into Eudragit S100 Preserving Mechanism of Cinnarizine Supersaturation. *AAPS PharmSciTech* **2022**, *23* (3), 80. https://doi.org/10.1208/s12249-022-02223-x.
(61) Morgan, E. M.; Lotfy, H. M.; Obaydo, R. H.; Fayez, Y. M.; Abdelkawy, M.; Boltia, S. A. Whiteness and Greenness Assessment with Efficacy Evaluation of Two UPLC Systems Applied for the Quantification of Cinnarizine and Dimenhydrinate along with Their Toxic Impurities. *Sustainable Chemistry and Pharmacy* **2023**, *36*, 101225. https://doi.org/10.1016/j.scp.2023.101225.
(62) Castro, G. A.; Coelho, A. L. L. R.; Oliveira, C. A.; Mahecha, G. A. B.; Oréfice, R. L.; Ferreira, L. A. M. Formation of Ion Pairing as an Alternative to Improve Encapsulation and Stability and to Reduce Skin Irritation of Retinoic Acid Loaded in Solid Lipid Nanoparticles. *International Journal of Pharmaceutics* **2009**, *381* (1), 77–83. https://doi.org/10.1016/j.ijpharm.2009.07.025.
(63) D. Ristroph, K.; K. Prud'homme, R. Hydrophobic Ion Pairing: Encapsulating Small Molecules, Peptides, and Proteins into Nanocarriers. *Nanoscale Advances* **2019**, *1* (11), 4207–4237. https://doi.org/10.1039/C9NA00308H.
(64) Heinen, C. A.; Reuss, S.; Amidon, G. L.; Langguth, P. Ion Pairing with Bile Salts Modulates Intestinal Permeability and Contributes to Food–Drug Interaction of BCS Class III Compound Trospium Chloride. *Mol. Pharmaceutics* **2013**, *10* (11), 3989–3996. https://doi.org/10.1021/mp400179v.
(65) Caram-Lelham, N.; Hed, F.; Sundelöf, L.-O. Adsorption of Charged Amphiphiles to Oppositely Charged Polysaccharides—A Study of the Influence of Polysaccharide Structure and Hydrophobicity of the Amphiphile Molecule. *Biopolymers* **1997**, *41* (7), 765–772. https://doi.org/10.1002/(SICI)1097-0282(199706)41:7<765::AID-BIP5>3.0.CO;2-N.
(66) Gaudana, R.; Parenky, A.; Vaishya, R.; Samanta, S. K.; Mitra, A. K. Development and Characterization of Nanoparticulate Formulation of a Water Soluble Prodrug of Dexamethasone by HIP Complexation. *Journal of Microencapsulation* **2011**, *28* (1), 10–20. https://doi.org/10.3109/02652048.2010.520093.
(67) Gaudana, R.; Gokulgandhi, M.; Khurana, V.; Kwatra, D.; Mitra, A. K. Design and Evaluation of a Novel Nanoparticulate-Based Formulation Encapsulating a HIP Complex of Lysozyme. *Pharmaceutical Development and Technology* **2013**, *18* (3), 752–759. https://doi.org/10.3109/10837450.2012.737806.
(68) Song, Y. H.; Shin, E.; Wang, H.; Nolan, J.; Low, S.; Parsons, D.; Zale, S.; Ashton, S.; Ashford, M.; Ali, M.; Thrasher, D.; Boylan, N.; Troiano, G. A Novel in Situ Hydrophobic Ion Pairing (HIP) Formulation Strategy for Clinical Product Selection of a Nanoparticle

Drug Delivery System. *Journal of Controlled Release* **2016**, *229*, 106–119. https://doi.org/10.1016/j.jconrel.2016.03.026.
(69) Weuts, I.; Kempen, D.; Verreck, G.; Peeters, J.; Brewster, M.; Blaton, N.; Van den Mooter, G. Salt Formation in Solid Dispersions Consisting of Polyacrylic Acid as a Carrier and Three Basic Model Compounds Resulting in Very High Glass Transition Temperatures and Constant Dissolution Properties upon Storage. *European Journal of Pharmaceutical Sciences* **2005**, *25* (4), 387–393. https://doi.org/10.1016/j.ejps.2005.04.011.
(70) Trasi, N. S.; Bhujbal, S. V.; Zemlyanov, D. Y.; Zhou, Q. (Tony); Taylor, L. S. Physical Stability and Release Properties of Lumefantrine Amorphous Solid Dispersion Granules Prepared by a Simple Solvent Evaporation Approach. *International Journal of Pharmaceutics: X* **2020**, *2*, 100052. https://doi.org/10.1016/j.ijpx.2020.100052.
(71) Neusaenger, A. L.; Fatina, C.; Yu, J.; Yu, L. Effect of Polymer Architecture and Acidic Group Density on the Degree of Salt Formation in Amorphous Solid Dispersions. *Mol. Pharmaceutics* **2024**. https://doi.org/10.1021/acs.molpharmaceut.4c00089.
(72) Mesallati, H.; Umerska, A.; Paluch, K. J.; Tajber, L. Amorphous Polymeric Drug Salts as Ionic Solid Dispersion Forms of Ciprofloxacin. *Mol. Pharmaceutics* **2017**, *14* (7), 2209–2223. https://doi.org/10.1021/acs.molpharmaceut.7b00039.
(73) Nie, H.; Su, Y.; Zhang, M.; Song, Y.; Leone, A.; Taylor, L. S.; Marsac, P. J.; Li, T.; Byrn, S. R. Solid-State Spectroscopic Investigation of Molecular Interactions between Clofazimine and Hypromellose Phthalate in Amorphous Solid Dispersions. *Mol. Pharmaceutics* **2016**, *13* (11), 3964–3975. https://doi.org/10.1021/acs.molpharmaceut.6b00740.
(74) Song, Y.; Yang, X.; Chen, X.; Nie, H.; Byrn, S.; Lubach, J. W. Investigation of Drug–Excipient Interactions in Lapatinib Amorphous Solid Dispersions Using Solid-State NMR Spectroscopy. *Mol. Pharmaceutics* **2015**, *12* (3), 857–866. https://doi.org/10.1021/mp500692a.
(75) Sarpal, K.; Tower, C. W.; Munson, E. J. Investigation into Intermolecular Interactions and Phase Behavior of Binary and Ternary Amorphous Solid Dispersions of Ketoconazole. *Mol. Pharmaceutics* **2020**, *17* (3), 787–801. https://doi.org/10.1021/acs.molpharmaceut.9b00970.
(76) Neusaenger, A. L.; Yao, X.; Yu, J.; Kim, S.; Hui, H.-W.; Huang, L.; Que, C.; Yu, L. Amorphous Drug–Polymer Salts: Maximizing Proton Transfer to Enhance Stability and Release. *Mol. Pharmaceutics* **2023**, *20* (2), 1347–1356. https://doi.org/10.1021/acs.molpharmaceut.2c00942.
(77) Moseson, D. E.; Tran, T. B.; Karunakaran, B.; Ambardekar, R.; Hiew, T. N. Trends in Amorphous Solid Dispersion Drug Products Approved by the U.S. Food and Drug Administration between 2012 and 2023. *International Journal of Pharmaceutics: X* **2024**, 100259. https://doi.org/10.1016/j.ijpx.2024.100259.
(78) Heller, J.; Baker, R. W.; Gale, R. M.; Rodin, J. O. Controlled Drug Release by Polymer Dissolution. I. Partial Esters of Maleic Anhydride Copolymers—Properties and Theory. *Journal of Applied Polymer Science* **1978**, *22* (7), 1991–2009. https://doi.org/10.1002/app.1978.070220720.
(79) Maghsoodi, M.; Nokhodchi, A.; Oskuei, M. A.; Heidari, S. Formulation of Cinnarizine for Stabilization of Its Physiologically Generated Supersaturation. *AAPS PharmSciTech* **2019**, *20* (3), 139. https://doi.org/10.1208/s12249-019-1338-7.
(80) Hsieh, Y.-L.; Ilevbare, G. A.; Van Eerdenbrugh, B.; Box, K. J.; Sanchez-Felix, M. V.; Taylor, L. S. pH-Induced Precipitation Behavior of Weakly Basic Compounds: Determination of Extent and Duration of Supersaturation Using Potentiometric Titration

and Correlation to Solid State Properties. *Pharm Res* **2012**, *29* (10), 2738–2753. https://doi.org/10.1007/s11095-012-0759-8.